Journal of the Serbian Chemical Society
JSCS-info@shd.org.rs • www.shd.org.rs/JSCS
J. Serb. Chem. Soc. 80 (3) 377–389 (2015)
JSCS–4723
UDC 662.75+662.61+66.023+544.4
Original scientific paper

Euler–Euler granular flow model of the combustion of liquid fuels in a fluidized reactor

STEVAN NEMODA[1]*, MILICA MLADENOVIĆ[1], MILIJANA PAPRIKA[1], DRAGOLJUB DAKIĆ[2], ALEKSANDAR ERIĆ[1] and MIRKO KOMATINA[3]

[1]*"Vinča" Institute of Nuclear Sciences, University of Belgrade, Belgrade, Serbia,* [2]*Innovation Center, Faculty of Mechanical Engineering, University of Belgrade, Belgrade, Serbia and* [3]*Faculty of Mechanical Engineering, University of Belgrade, Belgrade, Serbia*

(Received 30 January, revised and accepted 27 March 2014)

Abstract: This paper deals with the numerical simulation of liquid fuel combustion in a fluidized reactor using two-fluid Eulerian–Eulerian fluidized bed modeling incorporating the kinetic theory of granular flow (KTGF) to gas and solid phase flow prediction. The comprehensive model of the complex processes in a fluidized combustion chamber incorporates, besides the prediction of gas and particular phase velocity fields, the energy equations for the gas and solid phase and the transport equations of conservation of chemical species with the source terms due to the conversion of chemical components. Numerical experiments showed that the coefficients in the model of inter-phase interaction drag force have a significant effect, and they have to be adjusted for each regime of fluidization. A series of numerical experiments was performed with combustion of liquid fuels in a fluidized bed (FB), with and without significant water content. The given estimations were related to the unsteady state, and the modeled period corresponds to the passing time of the flow through the reactor column. The numerical experiments were conducted to examine the impact of the water content in a liquid fuel on the global FB combustion kinetics.

Keywords: computational fluid dynamics model; combustion; fluidized bed; two-fluid model; non-conventional fuel.

INTRODUCTION

Bubbling fluidized bed reactors with gas–solid particles is usually employed in industrial operations, such as energy production and petrochemical processes. Lately these reactors were repeatedly used for the thermal disintegration (incineration) of industrial waste and by-products. There are many benefits of fluidized bed combustion of unconventional fuels (with high amounts of water and other

* Corresponding author. E-mail: snemoda@vinca.rs
doi: 10.2298/JSC140130029N

ballast matter). The high thermal capacity of the fluidized bed, the thermal conductivity, and the intensity of heat transfer between the inert bed material and the fuel facilitates a stable combustion process of a wide variety of unconventional fuels, accompanied by a low sensitivity to fuel quality. The zone of intensive combustion occupies a relatively small volume, because most of the fuel burns in the bed itself, and burning-off in the "splash" zone and above the bed. In addition, FB furnaces operate at lower temperatures (≈ 850 °C) that are optimal from the aspect of decreased NO_x emission in the flue gases. Moreover, these furnaces are favorable from the viewpoint of the efficiency of in-bed desulfurization,[1] when it is necessary. For these reasons, this technology is recommended by the EU for waste matter combustion.

Experimental methods and numerical simulations are equally employed in research and development in the fields of energy and process engineering. The numerical models provide great opportunities for saving resources and time in the development of facilities and technologies in these fields. However, it should be noted that the numerical tools for simulation of complex processes, such as fluidized bed (FB) combustion, are not completely developed due to difficulties in describing complex two-phase flow and the specificity of heat and mass transfer in bubbling fluidized bed (BFB). In addition, many of existing numerical methods are not compliant to engineering needs, because they are complex and require expensive computer equipment, and are therefore not suitable for development and engineering applications.

There are two main approaches for computational fluid dynamics (CFD) modeling of gas–solid hydrodynamics. The first one is the Lagrangian–Eulerian modeling approach, also called discrete particle modeling (DPM), which solves the equations of motion individually for each particle, whereby the continuous phase is modeled using an Eulerian framework and the trajectories of the particles are simulated within a Lagrangian framework.[1–3] In large systems of particles, the Lagrangian–Eulerian model requires powerful computational resources because of the number of the equations that are to be solved. The second approach for modeling gas–solid flows is Eulerian–Eulerian modeling,[4–7] also called granular flow modeling (GFM), which assumes that both phases can be considered as fluids and takes the interpenetrating effect of each phase into consideration by using drag models. Consequently, the application of a proper drag model in Eulerian–Eulerian modeling is very important. The Eulerian two-fluid approach is an extension of the fluid dynamics formulation of single phase to multiphase flow. Particles in gas–solid flow may be treated as magnified molecules, and the analogy of their behavior to gas molecules is the reason for the wide use of the kinetic theory of granular flow (KTGF) for modeling the motion of particles. The KTGF approach is based on the concept of granular temperature. The granular temperature measures these random oscillations of the

particles and it is defined as the average of the three variances of the velocities of a particle. A full mathematical description of the kinetic theory is provided elsewhere.[8] In spite of detailed mathematical modeling of the complex processes in FB, the drag laws used in two-fluid models are semi-empirical in nature. Therefore, it is essential to use a drag law that correctly predicts the minimum fluidization conditions where the particles are in a state of suspension because of the balance between interfacial drag and body forces. The inter-phase interaction drag force model by Syamlal–O'Brien[9] is often used; the coefficient between fluid and solid (granular) phase in that model depends only on the phase void fraction, but not on the fluidization conditions.

In the present study, the GFM approach was chosen for the simulation because it requires less computational time and capacities. Here, the presented numerical experiments are related to engineering issues, for which detailed computations are not necessary. The different coefficients of the Syamlal–O'Brien inter-phase interaction drag force model were applied for the numerical simulation of a fluidized reactor, depending on the conditions of the fluidization.[10] The fluidization conditions were varied by applying different bubble fluidization intensities, bed particle sizes, gas composition, and temperature conditions. The investigation also includes numerical experiments of different regimes of liquid fuels combustion in a FB furnace for combustion of non-conventional liquid fuels. In this part, special attention was paid to the influence of the water content in the fuel on the position of the intense combustion zone and the global reaction rate.

Euler–Euler granular model of the fluidized bed

The Euler–Euler fluidized bed modeling approach considers the gas and FB dense phase (gas–particle system under conditions of the minimum fluidization) as two fluids with different characteristics. In the transport equations for transfer of momentum of the effective fluid (the FB dense phase), fluid–particle interactions under conditions of the minimum fluidization velocity were modeled, as well as the interaction between the particles themselves. In the Eulerian–Eulerian approach, all phases have the same pressure and that is the pressure of the continuous-primary phase. This model solves the continuity and momentum equations for each phase, and tracks the volume fraction. Furthermore, an additional transport equation for the granular temperature (which represents the fluctuating energy of the solids) is solved, and the bulk and shear viscosity of the solids are determined using the kinetic theory of gases on granular flow.

Moreover, it is necessary to define the coefficients for calculating the inter-phase interaction term. For modeling the interactions between gas and particle phases, within the suggested Euler–Euler granular approach to fluidized bed modeling, the routines incorporated in the modules of the commercial CFD software package Fluent 6.3.26 were used. This code allows for the presence of

several phases within one control volume of the numerical grid, by introducing the volume fraction of each phase. The solid phase represents a granular layer made of spherical particles of uniform diameter. The mass and momentum conservation equations are solved for each phase separately.

The basic and constitutive equations of the two-fluid granular model of a fluidized bed are given in Supplementary material to this paper.

NUMERICAL TESTS OF THE EULER–EULER GRANULAR MODEL FOR DIFFERENT FLUIDIZATION CONDITIONS

Despite rigorous mathematical modeling of the associated physics, the drag laws used in the model continue to be semi-empirical in nature. The semi-empirical procedure is proposed primarily for the prediction of drag law coefficients that correspond to real minimum fluidization conditions. The constants 0.8 and 2.65 in the coefficient *B* of the Syamlal–O'Brien inter-phase interaction drag force model (Eqs. (12) and (13) of the Supplementary material) are not universal, particularly when it comes to the fluidization regimes with a multi-component fluid and under non-isothermal conditions. For this reason, the presented numerical experiments were performed with 2D simulations of the fluidization columns with different particle diameters and for various temperatures and gas composition for fluidization, in order to analyze the influence of the various fluidization conditions on the choice of most suitable values of the coefficient B constants.

For the basic multiphase calculations, a professional package (Fluent 6.3.26) was used, but the inter-phase interaction drag force model (Eqs. (12) and (13) of the Supplementary material) were included in the calculation with their own code using the UDF options of Fluent.

The numerical solving of the governing equations of the Fluent Euler–Euler granular model (Eqs. (1)–(6) of the Supplementary material) was performed by the control volume method, whereby the coupling and correction of the velocity and pressure for multiphase flows are realized with the Phase Coupled SIMPLE (PCSIMPLE) algorithm. The discretisation of the convective terms was performed with the second-order upwind scheme.

The calculations were non-stationary, with a time step of 1 ms, which allowed a relatively quick convergence with a maximum of 100 iterations per time step, whereby the convergence criterion between two iterations was set to 10^{-3}. The number of time steps, *i.e.*, the total simulation time, was determined by the time required for the fluid to pass through the entire reactor space. The computational domain consisted of the two zones: layer of particles in the fluidized bed and the free flow above the fluidized bed. The entire numerical grid consisted of more than 13000 nodes.

The inter-phase interaction drag force, Eqs. (12) and (13) of the Supplementary material, were included in the numerical simulation process by the specialized subroutines in the "C" programming language ("user defined functions"), with which the user is able to upgrade individual parts of the core Fluent code.

The proposed Euler–Euler granular model of the fluidized bed was applied on the three fluidization regimes, the basic characteristics of which are presented in Table I. In all cases, the theoretical value of the fluidization number was approximately three. The default constants of 0.8 and 2.65 in the coefficient *B* (Eq. (13) of the Supplementary material) had to be changed for all three regimes. Accordingly, the appropriate constants used for the simulation of regime 1 were 0.282 and 9.077, respectively. The same constants, used for simulation of

regimes 2 and 3 had the values of 3.2 and 0.6625, respectively. The results of numerical simulations of treated fluidization regimes are presented in Fig. 1, which presents the distribution of the solid volume fraction during the development period of the bubbled fluidization.

TABLE I. Numerical simulation cases

Regime	Reactor dimensions m^2	FB height m	Particle size mm	Particle material density, kg m^{-3}	Fluidization gas	Inlet fluidization gas velocity m s^{-1}	T K
1	1×0.15	0.15	0.3	2600	Air	0.25	300
2	0.23×0.4	0.3	0.8	2400	Air	1	300
3	0.23×0.4	0.3	0.8	2400	Air multi-component	1	1200

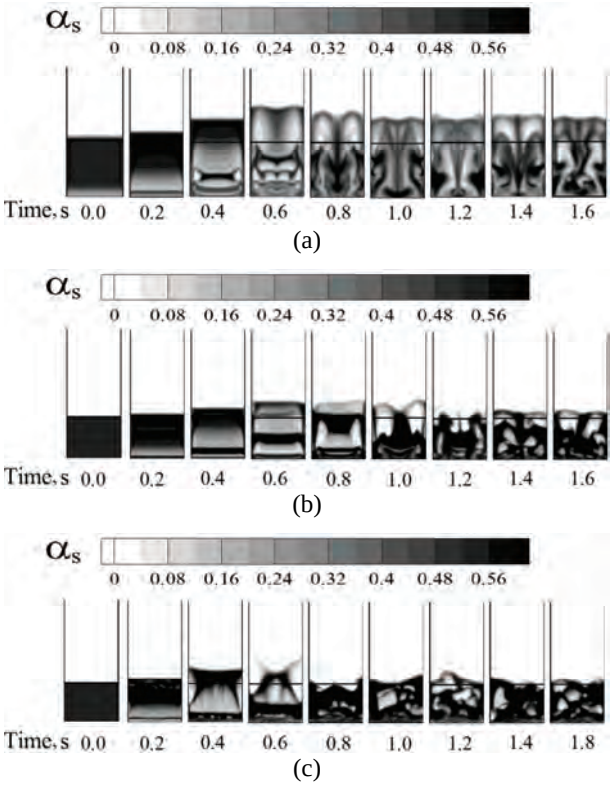

Fig. 1. Development of the solid volume fraction distribution for fluidization conditions in regimes: a) 1, b) 2 and c) 3.

2D simulation of combustion of liquid fuels in a fluidized combustion chamber

A comprehensive model of the complex processes in fluidized combustion chamber may be formed by upgrading of the proposed isothermal and single component Euler–Euler granular model of the fluidized bed, including the energy equation and the transport equations

of chemical species conservation with the source terms due to the conversion of chemical components. The additional equations for energy and conservation of chemical components are presented in Eqs. (1a), (1b) and (2):

Energy equation of the gas phase:

$$\frac{\partial}{\partial t}(\alpha_{\mathrm{g}}\rho_{\mathrm{g}}c_{p,\mathrm{g}}T_{\mathrm{g}})+\nabla(\alpha_{\mathrm{g}}\rho_{\mathrm{g}}\vec{u}_{\mathrm{g}}c_{p,\mathrm{g}}T_{\mathrm{g}})=\nabla\left(\frac{k_t}{c_{p,\mathrm{g}}}\nabla T_{\mathrm{g}}\right)+$$
$$+\nabla\left(\sum_i \alpha_{\mathrm{g}}\rho_{\mathrm{g}}D_{i,m}c_{p,i}T_{\mathrm{g}}\nabla Y_i\right)-h\left(T_{\mathrm{s}}-T_{\mathrm{g}}\right) \quad (1a)$$

Energy equation of the solid phase:

$$\frac{\partial}{\partial t}(\alpha_{\mathrm{s}}\rho_{\mathrm{s}}c_{p,\mathrm{s}}T_{\mathrm{s}})+\nabla(\alpha_{\mathrm{s}}\rho_{\mathrm{s}}\vec{u}_{\mathrm{s}}c_{p,\mathrm{s}}T_{\mathrm{s}})=\nabla\left(\frac{k_{\mathrm{s}}}{c_{p,\mathrm{s}}}\nabla T_{\mathrm{s}}\right)+h\left(T_{\mathrm{s}}-T_{\mathrm{g}}\right) \quad (1b)$$

Conservation equations for chemical components:

$$\frac{\partial}{\partial t}(\alpha_{\mathrm{g}}\rho_{\mathrm{g}}Y_i)+\nabla(\alpha_{\mathrm{g}}\rho_{\mathrm{g}}\vec{u}_{\mathrm{g}}Y_i)=\nabla\left(\alpha_{\mathrm{g}}\rho_{\mathrm{g}}D_{i,m}\nabla Y_i\right)+R_i \quad (2)$$

The energy balance equations for the two phases are connected through the interphase volumetric heat transfer coefficient (h), which was given by Gunn.[11] The granular conductivity coefficient has been determined using Syamlal and Gidaspow formulation.[12] Special attention was paid to the determination of the effective thermal conductivity of the gas and solid phase mixture.

The source term R_{i} in Eq. (2) corresponds to the chemical conversion rate of component i. The source term of the reaction rate for component i was defined using the Arrhenius expression:

$$R_i=k_{\mathrm{o},i}\exp\left(-\frac{E_{\mathrm{a},i}}{RT_{\mathrm{g}}}\right)\left[Y_i\right]^{a_1}\left[Y_j\right]^{a_2} \quad (3)$$

As the presented work is an integral part of extensive research of unconventional fuel combustion and industrial wastes incineration, diesel fuel ($C_{10}H_{22}$) with various water contents was used as the fuel in the processed numerical experiments. Accordingly, the list of chemical reactions that figure in treated test cases of the liquid fuels combustion in the FB, and the corresponding coefficients in the Arrhenius equation, Eq. (3), are given in Table II. The list includes two reactions that are not strictly chemical: the reactions of fuel devolatilization and the water evaporation. The basic coefficients for the kinetics reactions for the numerical experiments (Table II) were taken from the literature.[13,14]

TABLE II. Chemical reactions list

No.	Reaction	$-k_0$	E_{a} / J kmol^{-1}	a_1	a_2
1	$C_{10}H_{22(\mathrm{liquid})} \rightarrow C_{10}H_{22(\mathrm{vapor})}$	11.2	1.7E6	1	–
2	$C_{10}H_{22} + 10.5\ O_2 = 10CO + 11H_2O$	2.857E10	1.25E8	0.25	1.5
3	$CO + 0.5O_2 = CO_2$	1.0E12	1.0E8	1	1
4	$H_2O_{(\mathrm{liquid})} \rightarrow H_2O_{(\mathrm{vapor})}$	22.39	1.7E6	1	–

It should be noted that an actual quasi-three-phase system was treated here, that includes the liquid phase (water and fuel in liquid state at the inlet), the gas phase (air with flue gases: volatiles and steam) and the solid phase (inert bed particles). The numerical system was not really a three-phase one, since equations for only two phases were used: the fluid phase, consisting of the liquid fuel and water with gases (steam, volatiles, flue gasses and air) and the particle phase, which consisted of a granular layer (bed) of particles.

The presented numerical experiments were applied primarily for verification of the assumptions concerning the impact of the water content of a liquid fuel on the FB combustion intensity. In the experiments with a pilot furnace with liquid fuel feeding into the FB, withdrawal of the intense combustion zone was observed towards the areas below the bed surface during the combustion of liquid fuels with a significant water content, compared to those without water or with a low water content.[15,16] The emulsion of fuel (various oils) and water were prepared in special homogenizers (heated vessel with a stirrer and heated lines to the nozzle feeder). The detailed procedure is described elsewhere.[15,16] Based on these experimental results, it was concluded that the water in the fuel increased the global reaction rate of combustion in the fluidized bed furnace. This phenomenon is associated with a sudden transition of water in the fuel to steam while entering the heated FB (≈ 900 °C), which causes an expansion of the input jet and improved mixing of the fuel with oxidizer (air), as well as breakage of the liquid (still not vaporized) fuel into small droplets thereby increasing of the contact surface area of the fuel with the environment. The first attempts at numerical simulation of this phenomenon were reported earlier.[17]

The test case of numerical simulation of the processes in a fluidized combustion chamber was performed on the fluidization reactor of height 2.3 m and width of 0.4 m, as is shown in the schematic view of the reactor (Fig. 2). The modeled granular bed consisted of particles of diameter 0.8 mm and density of 2600 kg m^{-3}, where the height of the bed in the bulk condition was 0.3 m.

Fig. 2. Schematic view of the geometry of the numerically simulated fluidization reactor.

The fuel entered through a vertical nozzle placed axially on the bottom of the reactor. The nozzle for the introduction of the fuel was placed at a height of 0.05 m. Air for

fluidization was introduced annularly as is shown in Fig. 2. The inlet temperature of the air and fuel was ambient (300 K).

As was already mentioned, diesel ($C_{10}H_{22}$) with various contents of water was selected to be the test fuel. The presented numerical experiments were performed with 0.0, 0.1, 0.2, 0.3 and 0.4 mass fractions of water in the fuel. The inlet mass flow rate of air and the pure diesel fuel were 0.11627 and 0.002586 kg s^{-1}, respectively, in all calculations, which corresponded to an excess air ratio of λ = 3. In the cases when the fuel contained from 0.1 to 0.4 mass fraction of water, the inlet total fuel mass flows were 0.00287, 0.00323, 0.00370 and 0.00431 kg s s^{-1}.

THE RESULTS OF THE NUMERICAL SIMULATION OF LIQUID FUEL COMBUSTION IN THE FLUIDIZATION FURNACE

For the numerical experiments of the fluidized bed (FB) combustion, the calculation procedure and the numerical method were the same as for the cases treated in the numerical tests. The numerical grid shown in Fig. 2, consisting of 13130 nodes of which 3430 nodes were used for the granular bed zone, was employed.

The computational procedure consisted of two steps. In the first step of the calculation, the fluidization parameters were formed, according to the calculations presented in the numerical tests (Fig. 1c). The calculations were multicomponent and non-isothermal (the gas phase was heated up to 1200 K). The matrix values of the variables calculated in the first computing step were employed as the initial conditions for the second step of the calculation process. Moreover, in the second step, the boundary conditions were changed introducing the inlet fuel flow and the equations of chemical species with the source terms due to activation of the chemical reactions. Each of the steps comprised two simulation periods of approximately 2.5 s. After this period, it could be considered that the analyzed processes had entered a quasi-stationary state, because further changes were minor. Accordingly, in the second computing step, the processes were simulated from the beginning of the fuel introduction into the heated FB, under the developed fluidization conditions, up to the end of the period of 2.5–3 s.

The gas temperature distributions calculated by numerical simulation of diesel fuel combustion in fluidized bed under the specified conditions without moisture are shown in Fig. 3. for the period starting from 600 ms after fuel introduction into the heated fluidized bed. The temperature field in the zone of intense reaction in fluidized combustion chamber harmonically changed in time; hence, quasi-stationary processes could be assumed in this type of furnace.

The calculated temperature profiles along the fluidized reactor height for all five mass fractions of water from 0.0 to 0.4) are shown in Fig. 4. The temperature profiles were averaged over time for the period ranging from 2 to 3 s from the beginning of fuel feeding into the heated FB. The changes in the radial temperature profiles *versus* time were not symmetric, but stochastic; hence, the vertical

profiles in Fig. 4 represent the mass-weighted average temperature for the cross sections along the reactor height. The ordinate in Fig. 4 is the normalized temperature, defined as the ratio of the temperature and the maximal temperature (T_{max}) in corresponding conditions, while the abscissa represents the dimensionless height of the furnace, which is defined as ratio between the height of the reactor and the height of the fixed bed (H_{fb}). The temperature peaks and more rapid attaining of the maximum temperature in the given diagrams were shifted more towards the middle of the bed in the regimes with the fuel that contained water. It could be concluded that the water content in the fuel affects, to some degree, a withdrawal of the intense combustion zone in fluidized bed furnace towards the lower zones. This also pointed to the fact that with fuel that contained water, the location of combustion was lower, *i.e.*, that more efficient combustion was achieved. The registered effect of more a more rapid reaching of higher temperatures during combustion was more pronounced when the mass fractions of water in the fuel had values of 0.1 and 0.2, whereas for the higher moisture content in the fuel, this effect was less pronounced. This indicated the presence of a dual effect of the fuel moisture content, *i.e.*, on the one hand, the sudden expansion of water vapor improved the mixing of fuel and oxidizer, while the local heat balance was reduced on the other.

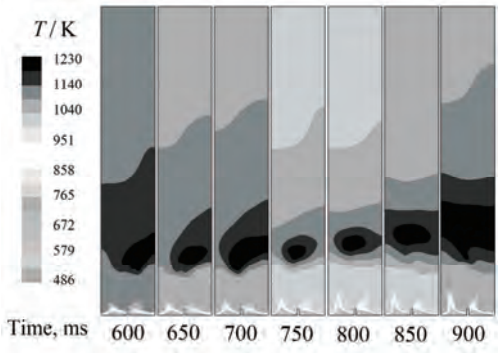

Fig. 3. The change in time of the temperature field in the fluidized combustion chamber.

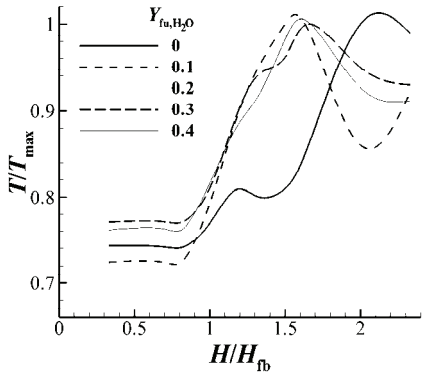

Fig. 4. Calculated temperature profiles along the fluidized reactor height for different mass fraction of water in the fuel.

The effect of the changing of combustion reaction rate due to the presence of water in the fuel could also be analyzed by using the diagram in Fig. 5, which shows the averaged values (in the combustion zone area) of the summary reaction kinetic rate depending on the water fraction in the fuel. These calculation results correspond to the conditions after a period of 2 s from the beginning of fuel feeding. Figure 5 shows that the mean reaction kinetic rate of diesel-fuel oxidation had higher values in the cases when the fuel contained water, whereby the dependency of the reaction rate on the moisture content in the fuel increased suddenly when the fraction of moisture was 0.1. The noted effect of the influence of fuel water content on the averaged fuel oxidation kinetic rate could be explained by the expansion of steam in the simulated FB, which in a number of nodes contributed to favorable (stoichiometric and over-stoichiometric) mixtures of fuel and oxidizer being obtained. On the other hand, higher values of the moisture content in the fuel led to a decrease in the local temperature of the FB, and then the reaction rates (according to the Arrhenius expression) were slightly lower.

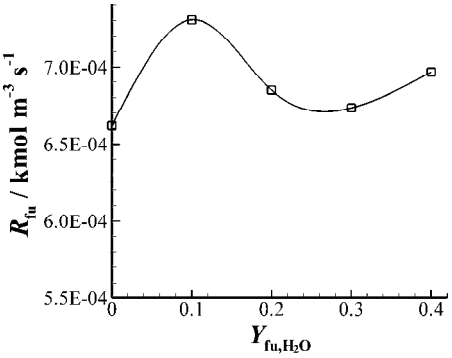

Fig. 5. Averaged kinetic rate of the summary reaction of diesel-fuel oxidation depending on the water content in the fuel.

CONCLUSIONS

A comprehensive 2D numerical model of the bubbled fluidized bed with combustion of liquid fuels has been proposed. The developed numerical model is based on Eulerian–Eulerian granular flow modeling with the kinetic theory of granular flow. It includes the following basic governing equations: the continuity equations of the solid and gas phase, the momentum conservation equations of the gas and solid phase, the energy equations of the gas and the solid phase and conservation equations for the chemical components.

For a more realistic simulation of events in the fluidized system of gas–solid particles that include combustion processes, it is necessary to adjust the constants of coefficient *B* (Eqs. (12) and (13) of the Supplementary material) depending on fluidization conditions and fluid and solid parameters. For this purpose, the proposed Euler–Euler granular model of the fluidized bed was applied on three different fluidization regimes.

The presented numerical experiments were primarily applied to an investigation of the impact of the water content in a liquid fuel on the intensity of FB combustion. The presented numerical experiments were performed with water mass fractions of 0.0, 0.1, 0.2, 0.3 and 0.4 in diesel fuel. Within the analysis of the results of the numerical simulation of FB combustion of the fuel with different water contents, the temperature profiles and the mean kinetic ratio of diesel fuel oxidation were considered.

The calculated vertical temperature profiles along the fluidized reactor height showed that the water content in the fuel affects, to some degree, the withdrawal of the intense combustion zone in the fluidized furnace towards the lower zones. Moreover, the averaged kinetic rate of diesel-fuel oxidation was higher when the fuel contained water. These two effects could be explained by an increase in the mixing intensity of the reactants and oxidizer due to steam expansion in the FB. Furthermore, the effect of the fuel moisture content had a dual nature: the sudden expansion of steam enhanced the mixing of fuel and oxidant, but also reduced the local thermal equilibrium; thus, the observed effect was less pronounced when the values of the water mass fraction in the fuel were higher than 0.1. Based on the analyzed results of the numerical experiments, it is could be concluded that liquid fuels burn efficiently in a fluidized bed, even if they contain a relatively large portion of water. When it comes to diesel fuel, with water mass fraction of 10 % had the most favorable kinetic characteristics, *i.e.*, fuel with 10 % of water by mass required less volume for the process of combustion in the FB.

SUPPLEMENTARY MATERIAL

The basic and constitutive equations of the two-fluid granular model of a fluidized bed are available electronically from http://www.shd.org.rs/JSCS/, or from the corresponding author on request.

NOMENCLATURE

a_1, a_2	rate exponent for the first and second reactant
C_D	drag coefficient
$c_{p,g}$, $c_{p,s}$	gas and solid specific heats
$D_{i,m}$	mass diffusion coefficient for species i
d_p, d_s	particle mean diameter
E_a	activation energy
e_s	restitution coefficient
g	gravity acceleration
g_{0s}	radial distribution function
h	heat transfer coefficient with specific surface
H	height
H_{fb}	height of the fixed bed
I	unity matrix
I_{2D}	second invariant of deviator of the strain rate tensor
K_{gs}	gas/solid momentum exchange

k_t thermal conductivity
k_o pre-exponential coefficient
$k_{\Theta s}$ diffusion coefficient for granular energy
p pressure
R universal gas constant
R_{fu} summary reaction rate
$\overline{\overline{S}}_k$ strain rate tensor
T absolute temperature
T_{max} maximal temperature in the regime
$\vec{u}$ instantaneous velocity vector
Y_i species mass fraction
Y_{fu,H_2O} water mass fraction in the fuel

Greek symbols

α phase void fraction
ρ density
λ bulk viscosity
$\overline{\overline{\tau}}$ phase stress–strain tensor
Θ_s granular temperature
$\mu_{s,kin}$ kinetic viscosity
$\mu_{s,coll}$ collisional viscosity
$\mu_{s,fr}$ frictional viscosity
ϕ angle of internal friction for the particle
ϕ_{gs} transfer rate of kinetic energy
$\gamma_{\Theta s}$ collisional dissipation energy

Indexes

b fluidized bed
g gas
s solid
i educts
j products

Acknowledgment. The authors wish to thank the Ministry of Education, Science and Technological Development of the Republic of Serbia for financing the project “Improvement of the industrial fluidized bed facility, within the scope of technology for energy efficient and environmentally feasible combustion of various waste materials in fluidized bed”, Project No. TR33042.

ИЗВОД

ДВОФЛУИДНИ ОЈЛЕР–ОЈЛЕРОВСКИ МОДЕЛ ГРАНУЛАРНОГ ТОКА САГОРЕВАЊА ТЕЧНОГ ГОРИВА У РЕАКТОРУ С ФЛУИДИЗОВАНИМ СЛОЈЕМ

СТЕВАН НЕМОДА[1], МИЛИЦА МЛАДЕНОВИЋ[1], МИЛИЈАНА ПАПРИКА[1], ДРАГОЉУБ ДАКИЋ[2], АЛЕКСАНДАР ЕРИЋ[1] и МИРКО КОМАТИНА[3]

[1]Институт за нуклеарне науке „Винча“, Универзитет у Београду, Београд, [2]Иновациони центар Машинског факултета, Универзитет у Београду, Београд и [3]Машински факултет, Универзитет у Београду, Београд

У раду је предложен модел нумеричке симулације сагоревања течних горива у флуидизованом слоју (FB), који се заснива на дво-флуидном Ојлер–Ојлеровском при-

ступу моделирања флуидизованог слоја уз одређивање поља брзина гаса и честица у двофазним грануларним токовима заснованог на аналогији са кинетичком теоријом гасова (RTGF). Свеобухватан модел комплексних процеса у флуидизационом ложишту подразумева, поред одређивања поља брзине гасне и честичне фазе, инкорпорирање енергетских једначина гасне и честичне фазе, као и транспортних једначина хемијских компоненти са изворним члановима који потичу од конверзије компонената. Нумерички експерименти показују да избор коефицијената у изразима за силе трења приликом интеракције фаза има изузетан значај и да се он мора спровести посебно за сваки значајно различит режим флуидизације. Урађене су серије нумеричких експеримената са симулацијом процеса сагоревања у FB, са и без значајног садржаја воде у гориву. Прорачуни су нестационарни, а моделирани временски период одговара времену за које гас прође целу висину реактора. Изложени нумерички експерименти су првенствено намењени за испитивање утицаја садржаја влаге у гориву на кинетику реакција у флуидизованом ложишту.

(Примљено 30. јануара, ревидирано и прихваћено 27. марта 2014)

REFERENCES

1. D. Gera, M. Gautam, Y. Tsuji, T. Kawaguchi, T. Tanaka, *Powder Technol.* **98** (1998) 3847
2. C. Ibsen, E. Helland, B. Hjertager, T. Solberg, L. Tadrist, R. Occelli, *Powder Technol.* **149** (2004) 29
3. G. A. Bokkers, M. van Sint Annaland, J. A. M. Kuipers, *Powder Technol.* **140** (2004) 176
4. A. Di Renzo, F. P. Di Maio, *Chem. Eng. Sci.* **62** (2007) 116
5. H. Enwald, E. Peiran, A. E. Almstedt, B. Leckner, *Chem. Eng. Sci*. **54** (1999) 311
6. L. Cammarata, P. Lettieri, G. D. M. Micale, D. Colman, *Int. J. Chem. Reactor Eng.* **1** (2003) 48
7. Y. Behjat, S. Shahhosseini, S. H. Hashemabadi, *Int. Commun. Heat Mass Transfer* **35** (2008) 357
8. D. Gidaspow, *Multiphase Flow and Fluidization: Continuum and Kinetic Theory Descriptions*, Academic Press, San Diego, CA, 1994, p. 30–320
9. M. Syamlal, T. J. O'Brien, *Int. J. Multiphase Flow* **14** (1988) 473
10. M. Syamlal, W. Rogers, T. J. O'Brien, *MFIX Documentation Theory Guide*, U.S. Department of Energy Office of Fossil Energy Morgantown Energy Technology Center, Morgantown, WV, 1993, p. 7
11. D. J. Gunn, *Int. J. Heat Mass Transfer* **21** (1978) 467
12. M. Syamlal, D. Gidaspow, *AIChE J.* **31** (1985) 127
13. O. G. Penyazkov, K. L. Sevrouk, V. Tangirala, N. Joshi, in *Proceedings of the Fourth European Combustion Meeting*, Vienna, Austria, 2009
14. J. F. Brennan, J. S. Shapiro, E. C. Watton, *J. Chem. Educ*. **51** (1974) 276
15. M. R. Mladenović, D. V. Dakić, S. Đ. Nemoda, R. V. Mladenović, A. M. Erić, M. J. Paprika, M. S. Komatina, in *Proceedings of 15th Symposium on Thermal Science and Engineering of Serbia*, Sokobanja, Serbia, 2011, CD-ROM, p. 490
16. M. R. Mladenović, M. J. Paprika, D. V. Dakić, S. Đ. Nemoda, A. M. Erić, M. S. Komatina, *Termotehnika* **38** (2012) 11 (in Serbian)
17. S. Nemoda, M. Mladenović, D. Dakić, M. Komatina, A. Erić, D. Đurović, In *Proceedings of International Conference Power Plants*, Zlatibor, Serbia, 2012, p. 1150.